# IDETC2017-68341

# A STUDY ON FINDING FINITE ROOTS FOR KINEMATIC SYNTHESIS

#### Mark M. Plecnik\*

Biomimetic Millisystems Lab Postdoctoral Scholar University of California Berkeley, California 94720 Email: mplecnik@berkeley.edu

### Ronald S. Fearing

Biomimetic Millisystems Lab
Department of Electrical Engineering and Computer Sciences
University of California
Berkeley, California 94720
Email: ronf@eecs.berkeley.edu

### **ABSTRACT**

This study presents new results on a method to solve large kinematic synthesis systems termed Finite Root Generation. The method reduces the number of startpoints used in homotopy continuation to find all the roots of a kinematic synthesis system. For a single execution, many start systems are generated with corresponding startpoints using a random process such that startpoints only track to finite roots. Current methods are burdened by computations of roots to infinity. New results include a characterization of scaling for different problem sizes, a technique for scaling down problems using cognate symmetries, and an application for the design of a spined pinch gripper mechanism. We show that the expected number of iterations to perform increases approximately linearly with the quantity of finite roots for a given synthesis problem. An implementation that effectively scales the four-bar path synthesis problem by six using its cognate structure found 100% of roots in an average of 16,546 iterations over ten executions. This marks a roughly six-fold improvement over the basic implementation of the algorithm.

# INTRODUCTION

The kinematic synthesis of (fairly simple) linkages often leads to polynomial systems that cannot be completely solved by today's methods. A common approach to avoid this problem is to reformulate equations in order to find some best linkage solution. Instead, direct solution of these equations can unveil a

diversity of designs otherwise not found. These solutions can be used to construct an atlas useful for exploring the space of design possibilities [1].

The state of the art technique for solving large polynomial systems is homotopy continuation. In this technique, a start system is continuously deformed to a target system. The roots of the start system (called startpoints) are already known or easily obtained, and are tracked across the homotopy to roots of the target system (endpoints). The use of continuation in kinematic synthesis was first performed by Roth and Freudenstein in 1963 [2]. During the next two decades, mathematicians matured this technique to construct homotopies with the same number of startpoints as the total degree [3], tracking in complex space to avoid path variable turning points [4], and tracking in projective space to compute roots at infinity and shorten paths [5]. From that point, improvements focused on limiting the number of paths to track while still finding all finite roots of polynomials by taking advantage of monomial structures [6-8]. More recently, Hauenstein et al. [9] developed a method that automatically simplifies equation structure.

It is often the case with kinematic polynomial systems of high degree that the very large majority of homotopy paths track to roots at infinity, which have no engineering relevance. To preclude this computational burden, we proposed the Finite Root Generation (FRG) method in [10]. FRG constructs homotopy startpoints in a manner such that all paths track to finite roots. As a trade-off, this opens up the possibility that a nonsingular root might be tracked more than once. Due to this, the calculation of

<sup>\*</sup>Address all correspondence to this author.

the number of paths required to solve a certain problem becomes probabilistic.

This work presents new results on FRG. In particular, the effect of scaling FRG for problems of different quantities of finite roots is characterized. This characterization suggests linear scaling for large quantities of roots, which is the case for the synthesis systems of interest. By focusing FRG on the collection of cognate sets rather than independent roots, a six-fold reduction of the four-bar path synthesis problem is achieved. As expected, the number of FRG iterations required to solve these equations decreased by roughly six as well, finding all roots in 16,546 FRG iterations on average over ten executions. If diminishing returns are avoided near the end of the algorithm, this technique finds 94.77% of roots on average in 4312 iterations. The results of FRG are applied to the kinematic synthesis of spined pinch gripper.

#### **FINITE ROOT GENERATION**

FRG was first introduced in [10]. The method uses polynomial homotopy continuation to find the roots of kinematic synthesis systems. FRG differs from the usual homotopy approach in that instead of constructing all the roots of a single start system, FRG constructs multiple start systems each with one root. The advantage being that these roots are constructed so that they track to finite roots of the target system, avoiding the burden of tracking a large number of roots at infinity. Although computations to infinity are easily handled by homogenizing equations to track paths in a projective space, these roots often comprise the far majority of computation. For the four-bar path synthesis problem, 97% of multihomogenenous homotopy paths are shown to track to infinity. Large numbers of infinite roots are usually due to a degeneration in the monomial structure from start system to target system, which is often the only option in multihomogeneous homotopy.

FRG homotopy paths are constructed by first generating a random mechanism of the desired topology to be synthesized. In kinematic synthesis, each root of a polynomial system represents a mechanism, and the system itself encodes a set of motion requirements. The randomly generated mechanism is a startpoint, and to construct a start system the motion of this mechanism is analyzed and encoded into a set of polynomials. This produces a single startpoint of a single start system with the important trait that its monomial structure matches that of the target system. Thus homotopy paths do not experience a degeneration and infinite paths are avoided. This is the major advantage of FRG.

Since the startpoint/start system construction process is random, this opens up the possibility that multiple FRG iterations might track to the same endpoint. The kinematic systems of interest have thousands of roots (or perhaps more) so that beginning FRG iterations have a low likelihood of repeating an endpoint. FRG applies to square systems with a finite number of

finite roots, so that as more unique roots are found the likelihood of finding another unique root decreases.

This leads to a situation of diminishing returns which is well modelled by the coupon collector problem from probability theory [11, p. 369]. That is, each FRG iteration can be termed a *trial* in which we pull a single sample randomly from a pool of unique roots with replacement. Assuming equal probability of happening upon any one root, to find n unique roots from a pool of N, the expected number of trials  $T_n$  is

$$T_n = \sum_{k=1}^n \frac{N}{N - (k-1)}. (1)$$

with a variance of

$$Var(T_n) = \sum_{k=1}^{n} \frac{N(k-1)}{(N-(k-1))^2}.$$
 (2)

# Scaling

By rearranging the summation of Eqn. (1), it can be written as the difference of harmonic numbers,

$$T_n = N\left(\left(\sum_{k=1}^N \frac{1}{k}\right) - \left(\sum_{k=1}^{N-n} \frac{1}{k}\right)\right),$$

$$\frac{T_n}{N} = H_N - H_{N-n}.$$
(3)

It is useful to obtain bounds on Eqn. (3). In [12], Young shows the inequality,

$$\frac{1}{2(N+1)} < H_N - \ln N - \gamma < \frac{1}{2N} \tag{4}$$

where  $\gamma$  is the Euler-Mascheroni constant. Applying Eqn. (4) to (3) obtains

$$\ln\left(\frac{N}{N-n}\right) - \frac{n}{2(N+1)(N-n+1)}$$

$$< \frac{T_n}{N} < \ln\left(\frac{N}{N-n}\right) - \frac{n}{2N(N-n)}.$$
 (5)

At this point it is useful to introduce the normalization substitutions

$$\hat{t} = \frac{T_n}{N}, \qquad \hat{n} = \frac{n}{N}, \tag{6}$$

where  $\hat{t}$  is the expected number of trials as a percentage of the total root count and  $\hat{n}$  is the percentage of the total number of roots. Eqn. (5) then takes the form

$$\ln\left(\frac{1}{1-\hat{n}}\right) - \frac{\hat{n}}{2(N+1)\left(1-\hat{n}+\frac{1}{N}\right)} < \hat{t} < \ln\left(\frac{1}{1-\hat{n}}\right) - \frac{\hat{n}}{2N(1-\hat{n})} \tag{7}$$

The right hand side of (7) is equivalent to an approximation of (3) derived from Euler's asymptotic expansion of  $H_N$ , see [13]. The expansion of (3) is

$$\hat{t} = \ln\left(\frac{1}{1-\hat{n}}\right) - \frac{\hat{n}}{2N(1-\hat{n})} + \sum_{k=1}^{\infty} \left(\frac{B_{2k}}{2k} \frac{1}{N^{2k}} \left(\frac{1}{(1-\hat{n})^{2k}} - 1\right)\right)$$
(8)

where  $B_{2k}$  denotes the  $2k^{\text{th}}$  Bernoulli number. This formulation suffers from the inability to evaluate the case of  $\hat{n}=1$ . To resolve this, note that harmonic numbers are related to the digamma function  $\Psi(\cdot)$  [14, Eqn. (1.12)], allowing (3) to be expressed as

$$\hat{t} = \Psi(N+1) - \Psi(N(1-\hat{n})+1).$$
 (9)

Furthermore the digamma function is defined for non-integer arguments. Eqn. (9) relates how many times  $\hat{t}$  more trials than the total number of roots N are expected in order to find  $\hat{n}$  percentage of roots. Fig. 1 illustrates that when  $\hat{n}$  is held fixed,  $\hat{t}$  tends toward a finite value as N tends toward infinity. By taking the limit of Eqn. (7) as  $N \to \infty$ , the asymptotes of Fig. 1 are computed as

$$\hat{t} = \ln\left(\frac{1}{1-\hat{n}}\right). \tag{10}$$

In fact, since we are only concerned with cases of large N, Eqn. (10) serves as an appropriate approximation of  $\hat{t}$ . This approximation is advantageous because it is independent of N so that it can be applied to estimations where the total root count is unknown. Furthermore, Eqn. (10) describes an approximate linear relationship between the total root count and the expected number of trials. To see this, substitute back in  $\hat{t} = \frac{T_n}{N}$ . For example, the target system studied in this paper reveals a solution structure that effectively reduces the number of roots to collect by six-fold. As a result, the expected number of trials to perform is approximately six-fold less. Linear scaling should be a desirable attribute for future applications.

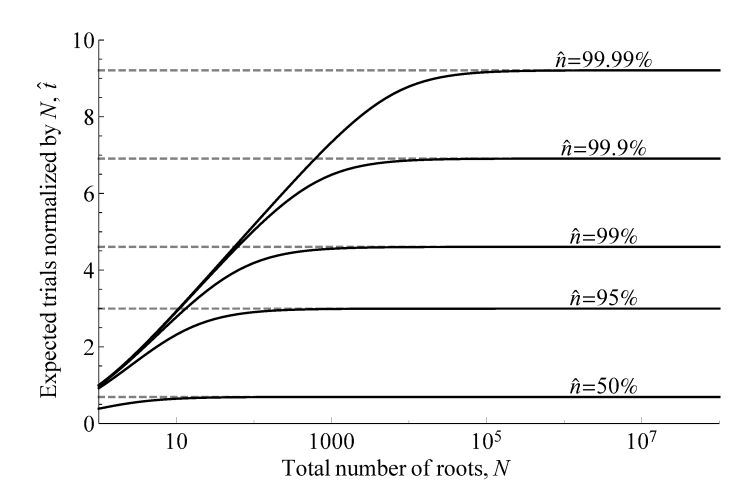


**FIGURE 1.** To obtain  $\hat{n}$  percent of N roots, it is expected that  $\hat{t}$  times N trials be performed. As N increases, the trial multiplier  $\hat{t}$  asymptotically approaches the lines defined in Eqn. (10).

#### **Estimation**

The quantities available for estimating the total root count N during an FRG computation are the n number of roots collected in-process and the  $T_n$  number of trials performed to collect those roots. Dividing the former by the latter defines the success ratio  $\alpha$ ,

$$\alpha = \frac{n}{T_n} = \frac{\hat{n}}{\hat{t}} \tag{11}$$

Substituting the approximation of Eqn. (10) into (11) obtains

$$\alpha = -\frac{\hat{n}}{\ln(1-\hat{n})}\tag{12}$$

The inverse of Eqn. (12) is

$$\hat{n} = \alpha W \left( -\frac{1}{\alpha} e^{-\frac{1}{\alpha}} \right) + 1. \tag{13}$$

where  $W(\cdot)$  is the principle branch of the Lambert function. Eqn. (13) provides an estimation of the percentage of roots obtained from the current success ratio.

## **METHODS**

In the proceeding sections, we characterize FRG by applying it several times to the four-bar path synthesis problem. Formulation of the kinematics of this system can be found in

[10]. The synthesis system includes eight polynomials in the unknowns  $\{A, B, C, D, \bar{A}, \bar{B}, \bar{C}, \bar{D}\}$  which are the isotropic coordinates [15] of four-bar pivots. Our usage of the overbar notation refers to complex conjugation in the case when isotropic coordinates define a two dimensional point. But for much of the solution process this is not the case, therefore barred and unbarred variables are treated as independent.

The motion requirement is for the four-bar to trace through task points  $(P_j, \bar{P}_j)$ ,  $j = 0, \dots, 8$ . The synthesis equations can be written compactly by first defining intermediate variables

$$\begin{aligned} & a = P_0 - C, & b_j = A - P_j, & f = C - A, \\ & c = P_0 - D, & d_j = B - P_j, & g = D - B, \\ & \mathbf{a} = \left\{ a(g\bar{g} - c\bar{c}), \, c(f\bar{f} - a\bar{a}), \, a, \, c \right\}^{\mathrm{T}}, \, \mathbf{c} = \left\{ a\bar{c}, \, \bar{a}c \right\}^{\mathrm{T}}, \\ & \mathbf{b}_j = \left\{ b_j, \, -d_j, \, -b_j d_j \bar{d}_j, \, b_j \bar{b}_j d_j \right\}^{\mathrm{T}}, & \mathbf{d}_j = \left\{ b_j \bar{d}_j, \, -\bar{b}_j d_j \right\}^{\mathrm{T}} \end{aligned}$$

$$\tag{14}$$

where overbar variables are defined symmetrically to those without. The synthesis equations are then

$$\mathbf{a}^T \bar{\mathbf{b}}_i \mathbf{b}_i^T \bar{\mathbf{a}} - \mathbf{c}^T \bar{\mathbf{d}}_i \mathbf{d}_i^T \bar{\mathbf{c}} = 0, \qquad j = 1, \dots, 8, \tag{15}$$

These equations have been shown to have 8652 roots [16]. Linkage cognate theory explains how for every four-bar that traces a certain coupler curve, there are two other four-bar linkages that trace that same curve [17]. Following this, for every solution to Eqn. (15), there can be generated two other solutions such that the set of three are

$$\mathbf{s}_{1} = \left\{ A, B, C, D, \bar{A}, \bar{B}, \bar{C}, \bar{D} \right\}, 
\mathbf{s}_{2} = \left\{ A, B', C', D', \bar{A}, \bar{B}', \bar{C}', \bar{D}' \right\}, 
\mathbf{s}_{3} = \left\{ B', B, C'', D'', \bar{B}', \bar{B}, \bar{C}'', \bar{D}'' \right\},$$
(16)

where

$$B' = \frac{(A-C)(D-P_0) - (B-D)(C-P_0)}{D-C} + P_0,$$

$$C' = A - C + P_0, \qquad D' = \left(\frac{A-C}{D-C}\right)(D-P_0) + P_0,$$

$$C'' = \left(\frac{B-D}{C-D}\right)(C-P_0) + P_0, \qquad D'' = B - D + P_0.$$
 (17)

with overbar variables defined symmetrically again. Furthermore, another symmetry in Eqn. (15) requires that solutions exist in pairs,

$$\mathbf{s} = \left\{ A, B, C, D, \bar{A}, \bar{B}, \bar{C}, \bar{D} \right\}$$

$$\mathbf{s}_{\text{sym}} = \left\{ B, A, D, C, \bar{B}, \bar{A}, \bar{D}, \bar{C} \right\}$$
(18)

**TABLE 1**. Quantity of roots found for each FRG run and how those roots organize into cognate sets.

	Qty. of in/complete cognate sets of size						Roots found		Cognate sets found	
Run	6	5	4	3	2	1	Qty.	Last on trial	Qty.	Last on trial
1	1441	1	0	0	0	0	8651	87549	1442	12026
2	1440	1	1	0	0	0	8649	97537	1442	12206
3	1438	2	1	1	0	0	8645	83169	1442	9485
4	1436	3	0	2	1	0	8639	97900	1442	14057
5	1438	1	3	0	0	0	8645	95088	1442	11780
6	1438	3	1	0	0	0	8647	67728	1442	13291
7	1435	3	2	2	0	0	8639	96957	1442	14389
8	1434	5	2	1	0	0	8640	93242	1442	52937
9	1436	4	2	0	0	0	8644	92540	1442	14662
10	1436	4	1	1	0	0	8643	88945	1442	10625

Together Eqns. (16)–(18) stipulate that every solution to (15) is a member of a set of six from which the whole set can be generated from any single member. The root set of Eqn. (15) consists of 1442 symmetric cognate sets.

The FRG algorithm was executed for five versions of Eqn. (15) two times each for a total of ten FRG runs. Each run performed 100,000 iterations. Each version of (15) was defined by a set of randomly generated target parameters  $P_j$ ,  $\bar{P}_j$ , j = 0, ..., 8, printed in the Appendix.

FRG startpoints were generated in the same manner as described in [10]. Homotopy paths were tracked using the BERTINI [18] path tracking software. If a homotopy path experienced a failure, usually from reaching a minimum step size, these trials were not included in the proceeding analysis. Path tracking failures occurred in 5.1% of paths.

# **RESULTS**

Of the ten FRG runs conducted in this study, none found all 8652 roots independently. However, all runs found at least one member of each of the 1442 cognate sets that comprise the full solution set. Since all roots of a cognate set are readily generated from a single member, the problem is effectively transformed to collecting 1442 coupons. These results are shown in Table 1. Using this cognate collecting strategy, FRG found 100% of roots in 16,546 trials on average. From Eqns. (1) and (2), FRG was expected to complete this calculation in 11,322 trials with a standard deviation of 1846 trials. The fastest FRG run beat this expectation by 1837 trials while the slowest run underperformed by

**TABLE 2**. The expected, actual, and estimated percentage  $\hat{n}$  of roots found for collecting 8652 independent roots or 1442 cognate sets. Results are displayed across all FRG runs at the points when 95% and 100% of roots were expected to be obtained. As well, estimates of the total quantity of roots N are displayed.

	Tracking 8562 roots						Tracking 1442 cognate sets						
	At trial 25922		At trial 83430			At trial	At trial 4312			At trial 11322			
	Expected $\hat{n} = 95\%$			Expected $\hat{n} = 100\%$			Expecte	Expected $\hat{n} = 95\%$			Expected $\hat{n} = 100\%$		
Run	Act. n	Est. <i>î</i>	Est. N	Act. $\hat{n}$	Est. <i>î</i>	Est. N	Act. $\hat{n}$	Est. <i>î</i>	Est. N	Act. n	Est. <i>î</i>	Est. N	
1	94.50	95.10	8598	99.95	99.99	8649	94.31	95.10	1430	99.86	99.96	1441	
2	94.64	95.07	8613	99.95	99.99	8649	95.35	94.90	1449	99.86	99.96	1441	
3	95.10	94.98	8663	99.92	99.99	8646	95.42	94.89	1450	100.00	99.96	1443	
4	95.58	94.89	8715	99.83	99.99	8638	94.94	94.98	1441	99.93	99.96	1442	
5	95.12	94.98	8665	99.91	99.99	8645	95.08	94.95	1444	99.93	99.96	1442	
6	95.32	94.94	8686	99.94	99.99	8648	94.11	95.13	1426	99.93	99.96	1442	
7	94.64	95.07	8613	99.83	99.99	8638	94.45	95.07	1433	99.93	99.96	1442	
8	94.89	95.02	8640	99.84	99.99	8639	94.66	95.03	1436	99.79	99.96	1440	
9	94.42	95.11	8589	99.90	99.99	8644	94.87	94.99	1440	99.93	99.96	1442	
10	94.72	95.05	8621	99.88	99.99	8643	94.52	95.06	1434	100.00	99.96	1443	

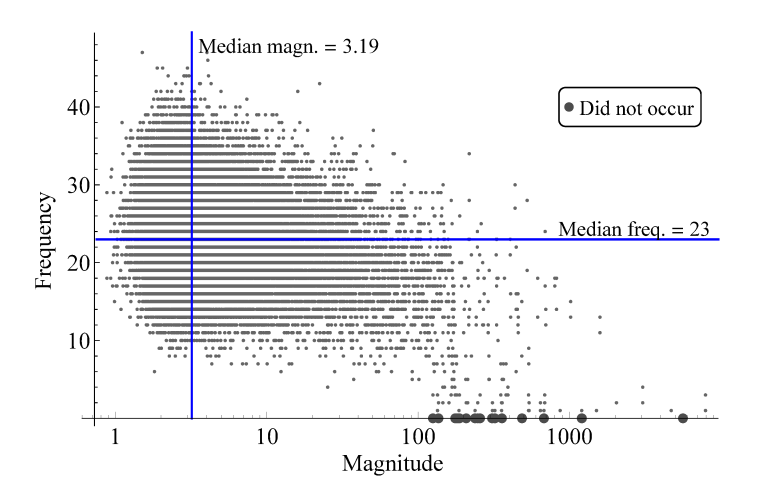


**FIGURE 2**. The frequency and magnitude of roots found in this study. Roots are compiled from five target systems over 200,000 FRG iterations each.

41,615 trials. This disparity in trials results from the high variance associated with finding the final few FRG roots. In actuality, all ten trials performed similarly as shown in Table 2.

Besides a roughly six-fold reduction in the number of iterations to perform, the cognate collecting implementation of FRG increased the likelihood of happening upon the final few roots. When collecting roots independently, there were between 1 and

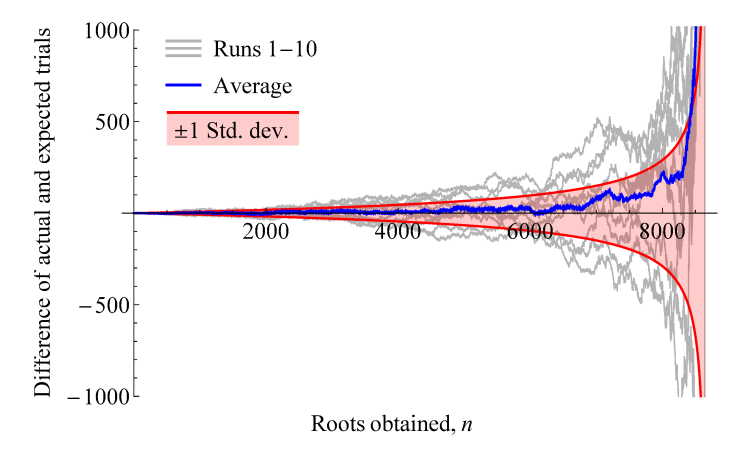


**FIGURE 3**. The difference between the actual and expected number of trials to obtain n roots. The shaded zone marks  $\pm 1$  standard deviation.

13 roots that FRG was unable to find. Of the five target systems defined by parameters in the Appendix, there were 1, 6, 3, 6, and 6 roots, respectively, that were not found after 200,000 iterations. These roots are plotted in Fig. 2 with the rest of roots against their magnitude and frequency of occurrence for all five target systems. This plot indicates a difficulty with finding roots of large magnitude.

As described in [10], FRG experiences acute diminishing returns collecting the final roots of a system, so it may not al-

ways make sense to invest this extra computational effort. For example, it is expected that 95% of roots are collected at 25,922 trials when roots are collected independently. Table 2 shows this is a very reasonable expectation. If cognate collecting is implemented, the expectation goes down to 4312 trials, roughly half the size of the original root set. On average, the difference between the actual and expected percentage of roots obtained was 0.37% at  $\hat{n}=95\%$  of roots. As  $\hat{n}$  increases, this tends error to decrease as shown for the  $\hat{n}=100\%$  cases in Table 2.

Table 2 also displays the in-process estimates of  $\hat{n}$  computed using the success ratio with Eqn. (13), which in turn estimates the total size N of the root set. Estimates improved as FRG advanced for both independently collected roots and the cognate collecting implementations.

The number of trials  $T_n$  to obtain the  $n^{\text{th}}$  root are compared to the expected number of trials in Fig. 3 by their difference plotted alongside  $\pm 1$  standard deviation as computed from Eqn. (2). The average of the ten runs indicates that FRG tends to require more trials than expected. The calculation of the expected number of trials (1) and variance (2) are based on the assumption that all roots are equally probable to appear at any trial. Conducting Pearson's chi-squared test on root frequencies indicates that this was not the case at a high significance level. Nonetheless, the estimations of Table 2 based on this assumption provide good accuracy.

# **EXAMPLE**

In order to demonstrate the usefulness of FRG for kinematic design, we apply the results of this study to the design of a spined pinch gripper. The motion task is to guide two spine tips to move inwards as a gripper mechanism moves down toward the ground. In a frame fixed to the gripper, this corresponds to mirrored curves that move upwards then inwards. We choose to design one half of the gripper to guide a spine tip through the points

$$\begin{split} P_0 &= 0.000000 + 1.00000i, & P_1 &= 0.129939 + 0.948025i, \\ P_2 &= 0.251380 + 0.891794i, & P_3 &= 0.359164 + 0.816847i, \\ P_4 &= 0.445855 + 0.701280i, & P_5 &= 0.498510 + 0.552674i, \\ P_6 &= 0.528574 + 0.364258i, & P_7 &= 0.538599 + 0.187021i, \\ P_8 &= 0.536284 + 0.0000000i. \end{split}$$

These points were substituted into Eqn. (15) which was then solved with a parameter homotopy. The complete root set found from FRG run 1 served as the startpoints from which the parameter homotopy was constructed. The parameter homotopy tracked to 270 linkage solutions i.e. solutions in which  $(A,\bar{A})$ ,  $(B,\bar{B})$ ,  $(C,\bar{C})$ , and  $(D,\bar{D})$  are complex conjugate pairs. These solutions were organized into 45 symmetric cognate sets of 6. Because of the symmetry described in (18), these solutions correspond to 135 linkage design candidates.

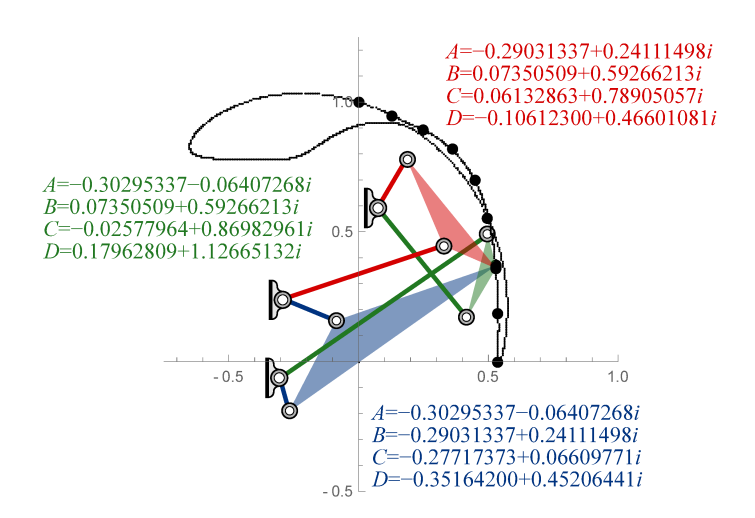


**FIGURE 4**. A set of cognate linkages that trace through the task points, albeit with pivots in unacceptable locations.

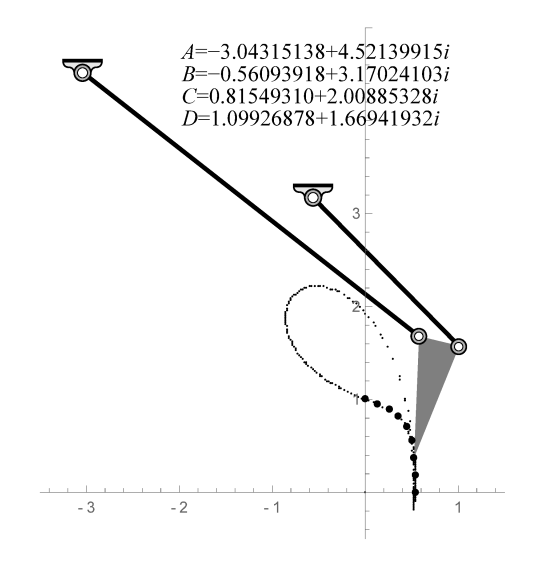


**FIGURE 5**. A linkage design candidate appropriate for a spined pinch gripper.

An example of cognate linkage solutions is given in Fig. 4. The three four-bars depicted trace identical coupler curves. If all three coupler points were pinned together the overconstrained mechanism would still move with mobility one. Most linkage solutions from this example had pivots in locations similar to Fig. 4, which is not useful for the gripper design at hand.

However, by virtue of obtaining a large solution base, a few solutions had pivots at more appropriate locations, including the design shown in Fig. 5. An embodiment of this design and its motion from a global frame are shown in Fig. 6. This embodiment uses living hinges to connect two rocker links to the cou-

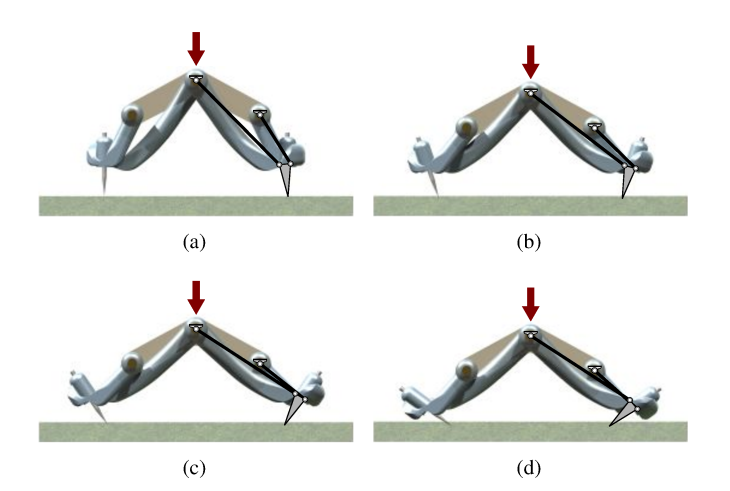


**FIGURE 6.** An embodiment of the design from Fig. 5 and its motion from a global frame. As the body of the gripper moves toward the ground, the spine tips at first move upward towards the body, then curl inwards to create a pinching motion

pler link which holds the spine tips in position. As the body of the gripper moves toward the ground, the spine tips at first move upward towards the body, then curl inwards.

#### CONCLUSION

The new results contained in this study include a characterization of how FRG scales with problem size, a demonstration of problem reduction informed by linkage cognate structures, and the application of FRG results to the design of a spined pinch gripper. Linear scaling with respect to problem size was concluded by analyzing the probabilistic model of root collection as the total root set size tended toward infinity. This uncovered an approximate linear scaling law which is valid for the large problems we are interested in. Following this result, we demonstrated an implementation of FRG that effectively scaled down the fourbar path synthesis problem by six using the cognate structure of the synthesis solutions. FRG was executed ten times on this problem to characterize its basic implementation versus an implementation which focuses on the collection of cognate sets. Besides substantially decreasing the required number of FRG iterations, the latter showed an increased ability to collect the final roots and estimate the final size of the root set. The results of this study were applied to the kinematic synthesis of a spined pinch gripper mechanism. In future work, we hope to apply FRG to more complex problems.

### **ACKNOWLEDGMENT**

The authors gratefully acknowledge the support of National Science Foundation award CMMI-1636302. Any opinions, find-

ings, and conclusions or recommendations expressed in this material are those of the authors and do not necessarily reflect the views of the National Science Foundation.

#### **REFERENCES**

- [1] Plecnik, M., Haldane, D. W., Yim, J. K., and Fearing, R. S., 2016. "Design exploration and kinematic tuning of a power modulating jumping monopod". *Journal of Mechanisms and Robotics*, *9*(1), p. 011009.
- [2] Roth, B., and Freudenstein, F., 1963. "Synthesis of pathgenerating mechanisms by numerical methods". *Journal of Engineering for Industry*, **85**(3), pp. 298–304.
- [3] Chow, S., Mallet-Paret, J., and Yorke, J. A., 1979. *A Homotopy Method for Locating All Zeros of a System of Polynomials*, Vol. 730 of *Lecture Notes in Mathematics*. Bonn, Germany, pp. 77–88.
- [4] Zangwill, W. I., and Garcia, C. B., 1981. *Pathways to Solutions, Fixed Points, and Equilibria*. Prentice-Hall, Englewood Cliffs, NJ.
- [5] Morgan, A. P., 1987. Solving Polynomial Systems Using Continuation for Engineering and Scientific Problems. Prentic-Hall, Englewood Cliffs, NJ.
- [6] Morgan, A. P., and Sommese, A. J., 1987. "A homotopy for solving general polynomial systems that respects m-homogeneous structures". *Applied Mathematics and Computation*, *24*(2), pp. 101–113.
- [7] Su, H., McCarthy, J. M., and Watson, L. T., 2004. "Generalized linear product homotopy algorithms and the computation of reachable surfaces". *Journal of Computing and Information Science in Engineering*, **4**(3), pp. 226–234.
- [8] Verschelde, J., Verlinden, P., and Cools, R., 1994. "Homotopies exploiting Newton polytopes for solving sparse polynomial systems". *SIAM Journal on Numerical Analysis*, *31*(3), pp. 915–930.
- [9] Hauenstein, J. D., Sommese, A. J., and Wampler, C. W., 2011. "Regeneration homotopies for solving systems of polynomials". *Mathematics of Computation*, 80(273), pp. 345–377.
- [10] Plecnik, M., and Fearing, R. S., 2017. "Finding only finite roots to large kinematic synthesis systems". *Journal of Mechanisms and Robotics*, *9*(2), p. 021005.
- [11] Parzen, E., 1960. *Modern Probability Theory and Its Applications*. John Wiley & Sons, Inc, New York.
- [12] Young, R. M., 1991. "Euler's constant". *The Mathematical Gazette*, **75**(472), pp. 187–190.
- [13] Mortici, C., and Villarino, M. B., 2015. "On the Ramanujan–Lodge harmonic number expansion". *Applied Mathematics and Computation*, *251*, pp. 423–430.
- [14] Rassias, T. M., and Srivastava, H. M., 2002. "Some classes of infinite series associated with the Riemann zeta and polygamma functions and generalized harmonic num-

- bers". *Applied Mathematics and Computation*, 131(2–3), pp. 593–605.
- [15] Wampler, C. W., 1996. "Isotropic coordinates, circularity, and Bézout numbers: planar kinematics from a new perspective". In Proceedings of the ASME 1996 DETC/CE Conference.
- [16] Wampler, C. W., Sommese, A. J., and Morgan, A. P., 1992. "Complete solution of the nine-point path synthesis problem for four-bar linkages". *Journal of Mechanical Design*, *114*(1), pp. 153–159.
- [17] Roberts, S., 1875. "Three-bar motion in plane space". *Proceedings of the London Mathematical Society,* s1-7(1), pp. 14–23.
- [18] Bates, D. J., Hauenstein, J. D., Sommese, A. J., and Wampler, C. W. "Bertini: Software for numerical algebraic geometry". Available at bertini.nd.edu with permanent doi: dx.doi.org/10.7274/R0H41PB5.

# **Appendix: Target Parameters**

**TABLE 3**. Parameters used to define the target systems in this study.

Target Parameters 1	Target Parameters 2	Target Parameters 3
$P_0 = 0.776874 - 0.642684i$	0.445812-0.860398i	-0.379870 + 0.803287i
$P_1$ 0.549479+0.418241 $i$	-0.151041 + 0.521027i	0.921351+0.483121 <i>i</i>
$P_2 -0.261986 -0.403618i$	-0.897116 + 0.185952i	-0.831159 + 0.059860i
P <sub>3</sub> 0.767234-0.378801 <i>i</i>	0.511317 - 0.028132i	0.477860 + 0.626925i
$P_4 -0.068090 +0.919907i$	-0.639865 - 0.306563i	-0.334216 - 0.224893i
$P_5 = 0.055654 + 0.675009i$	-0.998164 + 0.275757i	-0.172764 - 0.461834i
$P_6 -0.134960 -0.424099i$	0.307952 - 0.580697i	-0.567299 + 0.718201i
$P_7 = -0.239858 + 0.041043i$	-0.204723 - 0.681984i	0.798680 + 0.008829i
P <sub>8</sub> 0.635501-0.474101 <i>i</i>	-0.545189 - 0.224840i	-0.818067 - 0.509198i
$\bar{P}_0$ 0.873111+0.292468 $i$	-0.706916 - 0.481828i	0.114622 + 0.381387i
$\bar{P}_1$ 0.689034 $-$ 0.944901 $i$	-0.253584 + 0.187983i	-0.557820 + 0.159911i
$\bar{P}_2$ 0.854109 $-0.482044i$	0.259632 - 0.036125i	0.522259 + 0.748322i
$\bar{P}_3 -0.268805 -0.865098i$	-0.222836 + 0.103006i	-0.989851 - 0.175180i
$\bar{P}_4$ -0.263339-0.451987 $i$	0.992221 + 0.249885i	-0.815471 - 0.222604i
$\bar{P}_5$ -0.221326+0.775947 $i$	-0.726627 - 0.731216i	-0.577187 - 0.246342i
$\bar{P}_6$ 0.165736+0.319065 <i>i</i>	0.937814 + 0.561564i	-0.810094 - 0.623226i
$\bar{P}_7$ 0.248468+0.077381 $i$	0.713889 + 0.886674i	-0.932418 + 0.479788i
$\bar{P}_8$ 0.342355-0.501518 <i>i</i>	0.995395-0.173441 <i>i</i>	-0.053098 - 0.389105i
Target Parameters 4	Target Parameters 5	
$P_0$ 0.766574 $-$ 0.303366 $i$	-0.603732 - 0.726926i	
$P_1 -0.169761 -0.094169i$	-0.474312 - 0.227178i	
$P_2$ 0.803894+0.702355 <i>i</i>	-0.593796 + 0.947155i	
$P_3$ 0.190963 $-$ 0.211693 $i$	-0.580044 - 0.085847i	
$P_4 - 0.756797 - 0.761911i$	0.477049 - 0.048159i	
P <sub>5</sub> 0.252935-0.738818 <i>i</i>	0.604987 - 0.205613i	
$P_6 -0.004816 -0.564282i$	0.472113-0.646370 <i>i</i>	
$P_7 = 0.090282 - 0.769713i$	0.817195-0.159517 <i>i</i>	
$P_8 -0.919597 +0.539628i$	-0.468734 - 0.774642i	
$\bar{P}_0$ 0.043183+0.183683 $i$	0.495074 + 0.091227i	
$\bar{P}_1$ 0.419272+0.516355 <i>i</i>	-0.089742 - 0.642176i	
$\bar{P}_2$ 0.572342+0.485196 <i>i</i>	-0.098454 - 0.458862i	
$\bar{P}_3$ 0.570356-0.741328 <i>i</i>	-0.305446 + 0.932913i	
$\bar{P}_4$ 0.485626+0.709176 <i>i</i>	-0.047797-0.320071 <i>i</i>	
$\bar{P}_5$ 0.320779 $-0.848190i$	0.337652+0.973372 <i>i</i>	
	0.500576 0.200120:	
$\bar{P}_6$ 0.951927+0.164502 $i$	-0.589576-0.380130 <i>i</i>	
$P_6 = 0.951927 + 0.164502i$ $\bar{P}_7 = -0.175106 + 0.237662i$ $\bar{P}_8 = 0.308168 - 0.769707i$	-0.364004 + 0.843730i $-0.867954 + 0.810325i$	